Synthetic Metals 159 (2009) 595–603

Contents lists available at ScienceDirect

Synthetic Metals

journal homepage: www.elsevier.com/locate/synmet

Conducting polymer functionalized multi-walled carbon nanotubes with noble metal nanoparticles: Synthesis, morphological characteristics and electrical properties

Kakarla Raghava Reddy[a], Byung Cheol Sin[a], Kwang Sun Ryu[a], Jin-Chun Kim[b], Hoeil Chung[c], Youngil Lee[a,*]

[a] Department of Chemistry, University of Ulsan, Moogeo-dong Nam-gu, Ulsan 680-749, Republic of Korea
[b] School of Materials Science and Engineering, University of Ulsan, Ulsan 680-749, Republic of Korea
[c] Department of Chemistry, Hangyang University, Seoul 133-791, Republic of Korea

ARTICLE INFO

Article history:
Received 18 June 2008
Received in revised form 3 November 2008
Accepted 28 November 2008
Available online 16 January 2009

Keywords:
Carbon nanotubes
Conducting polymer
Metal nanoparticles
Nanocomposites
Functionalization

ABSTRACT

We report the synthesis of conducting polyaniline-functionalized multi-walled carbon nanotubes (MWCNTs-*f*-PANI) containing noble metal (Au and Ag) nanoparticles composites (MWCNTs-*f*-PANI-Au or Ag-NC). MWCNTs-*f*-PANI was initially synthesized by functionalizing acyl chloride terminated carbon nanotubes (MWCNTs-COCl) with 2,5-diaminobenzenesulphonic acid (DABSA) via amide bond formation, followed by surface initiated *in situ* chemical oxidative graft polymerization of aniline in the presence of the ammonium persulphate (APS) as an oxidizing agent. MWCNTs-*f*-PANI was then dispersed into an aqueous Au or Ag metal salt solution followed by the addition of sodium citrate, which acted as a reducing agent. The resulting composite contained a high level of well dispersed Au or Ag nanoparticles (MWCNTs-*f*-PANI/Au-NC or MWCNTs-*f*-PANI-Ag-NC). Morphological and structural characteristics, as well as electrical conducting properties of the hybrid nanocomposites were characterized using various techniques including high resolution transmission electron microscopy (HRTEM), X-ray diffraction (XRD), Fourier transform infrared spectroscopy (FT-IR), UV–visible spectroscopy (UV–vis) and four-probe measurements. FT-IR spectra confirmed that PANI was covalently bonded to MWCNTs. TEM images revealed the presence of Au or Ag nanoparticles finely dispersed in the composites with a size of <15 nm. XRD analysis revealed the presence of strong interactions between the metal nanoparticles and MWCNTs-*f*-PANI, where the metal particles were present in a phase-pure crystalline state with face centered cubic (fcc) structure. The room temperature electrical conductivity of the MWNCTs-*f*-PANI/Au or Ag composites was 4.8–5.0 S/cm, respectively, which was much higher than that of CNTs-*f*-PANI (0.18 S/cm) or pure PANI (2.5×10^{-3} S/cm). A plausible mechanism for the formation of nanocomposites is presented. We expect that the new synthesis strategy reported here will be applicable for the synthesis of other hybrid CNTs–polymer/metal nanocomposites with diverse functionalities. This new type of hybrid nanocomposite material may have numerous applications in nanotechnology, gas sensing, and catalysis.

1. Introduction

The discovery of carbon nanotubes (CNTs) by Iijima in 1991 has attracted scientific and technological interest worldwide. Both multi-walled and single-walled carbon nanotubes (MWCNTs and SWCNTs) have excellent chemical, thermal, and mechanical properties in terms of their stiffness, high Young's modulus, flexibility, and high electrical conductivity [1–4]; these properties can be attributed to the high degree of organization and high aspect ratio of CNTs. CNTs exhibit remarkable properties useful for constructing nanoscale devices and developing multifunctional composite materials [5,6]. However, owing to the rigidity, chemical inertness, and strong π–π interactions of nanotubes, pure CNTs cannot be processed, as they are difficult to dissolve or disperse in common organic solvents or polymeric matrices. Therefore, the side walls of CNTs must be chemically modified to improve their dispersion or solubility in solvents or polymers [7–9]. Recently, the modification of many materials utilizing CNTs has attracted considerable interest, owing to the outstanding properties of CNTs [10–12]. Based on interactions between organic and inorganic materials in such hybrids, a large number of new hybrid nanocomposite (NC) materials with synergetic behaviors and potential applications in electronic or nanoelectronic devices have been obtained. Of these hybrids, CNT-conducting electroactive polymer (CEP) composites

* Corresponding author. Tel.: +82 52 259 2341; fax: +82 52 259 2348.
E-mail address: nmryil@ulsan.ac.kr (Y. Lee).

0379-6779/$ – see front matter.
doi:10.1016/j.synthmet.2008.11.030

are one of the most important, based on their electron donor and acceptor interactions.

Research on the precise control of synthesis of composite nano-structures has become increasingly important as the functionality, processability, size, and morphology of nano-structures play a crucial role in the development of CEP-CNTs/metal hybrid nanocomposites for potential applications as sensors, supercapacitors, electromagnetic interference shielding materials, and catalysts [13–16]. Composites of CNTs with CEPs such as polyaniline, polypyrrole, and polythiophene have been prepared by *in situ* chemical polymerization, electro-polymerization or irradiation methods [17–20]; however, composites synthesized using these methods have several disadvantages including the tendency to form aggregate granular shapes when CNTs are present in the composite, lack of colloidal stability, and poor general characteristics.

The interactions between CNTs and a CEPs matrix in the composites prepared by above methods are electrostatic or physical adsorption. So, it is easy to destroy such poor interactions between them due to the absence of strong covalent bonds. Strong bonding is essential to ensure efficient transfer from the CEP matrix to the carbon nanotube lattice, and is thus one of the critical issues currently related to CNTs–CEP composites. Given the importance of such composites, methods need to be developed for the synthesis of chemically functionalized CNTs–polymer composites before they can used for technological applications. Specifically, chemical functionalization leads to enhancement of both processability and performance of the resulting composite material.

Many recent efforts have focused on the synthesis of CEPs with metal and metal oxides (such as Fe_3O_4, TiO_2, SiO_2, V_2O_5, Cu, Pd, Ag and Pt) because of their superior performance as rechargeable batteries, nanodevices, hydrogen storage vessels, nonvolatile memory units, and chemical and biological sensors, among others [21–26]. There are two general methods that used to synthesize CEPs-metal nanoparticles composites, namely chemical (*in situ*/*ex situ*), and electrochemical polymerization. In the *in situ* method, metal particles are incorporated within CEP matrix by the reduction of metallic precursor ions; whereas *ex situ* method involves preparation of metal nanoparticles at the first, followed by the dispersion into the CEP matrix. The electrochemical method involves through incorporation of metal particles during the electrosynthesis of the polymer or by the electrodeposition of metal particles on preobtained CEPs. Polyaniline (PANI) is the most important CEP because of its low cost, high polymerization yield, moderate electrical conductivity, good environmental stability, mechanical flexibility, reversible acid/base doping/dedoping nature, and its potential use in a large variety of applications [27,28]. Notwithstanding, the conductivity and current carrying capacity of PANI are lower compared to those of most metals; this deficit could be addressed by incorporating metal particles into a polymer matrix.

Noble metal (such as Au and Ag)-containing nanoparticles have received a great deal of attention due to their unique electrical, catalytic, optical and sensing characteristics as well as their potential use in a wide variety of applications ranging from optical and electronic nanodevices to biosensing and antimicrobial agents [29,30]. Composites of PANI and its derivatives with Au or Ag nanoparticles have been synthesized via spontaneous redox reaction of corresponding monomers with $AuCl_3$ or $AgNO_3$ using a one step polymerization method where the monomer acts as reductant of the metal ions [31,32]. The composite obtained by this method has some disadvantages; for example, the binding between the organic and inorganic counterparts is weak, control of size and shape is difficult, and composite particles form heavy agglomerates. Hence, dispersion of uniform metal nanoparticles into polymers has become an important issue in the fabrication of desirable polymer nanocomposites; however, despite their importance, reports of hybrid composites with three components composed of chemically functionalized CNTs with CEPs and well dispersed metal nanoparticles are scarce.

In this article, we report a new strategy for the synthesis of hybrid nanocomposites consisting of MWCNTs functionalized with PANI (MWCNTs-*f*-PANI) and noble metal (Au and Ag) nanoparticles. Firstly, MWCNTs-*f*-PANI was prepared. For this we modified the carbon nanotubes (MWCNTs-COCl) with DABSA via amide linkage, and subsequently *in situ* chemical oxidative graft polymerization of aniline was performed. Next, Au or Ag nanoparticle-embedded MWCNTs-*f*-PANI was prepared by dispersing MWCNTs-*f*-PANI in an aqueous Au or Ag salt solution followed by sodium citrate reduction. The resulting MWCNTs-*f*-PANI/Au or MWCNTs-*f*-PANI/Ag nanocomposites were investigated in detail using HRTEM, XRD, FT-IR, UV–vis and electrical conductivity measurements. The synthesized hybrid composites possessed high conductivity. The formation mechanism of the nanocomposites is also presented.

2. Experimental

2.1. Materials

The MWCNTs used in this work were purchased from nanocarbon Co., Ltd. Aniline, thionylchloride ($SOCl_2$), 2,5-diaminobenzenesulphonic acid (DABSA), $HAuCl_4{\cdot}H_2O$, $AgNO_3$ and ammonium persulphate (APS) were obtained from Aldrich and were used as received.

2.2. Chemical oxidation of MWCNTs

Typically, 1.0 g of crude MWCNTs were added to 150 mL of HNO_3:H_2SO_4 (1:3, v/v) and sonicated for 4 h in an ultrasonic bath (40 kHz); the resulting mixture was then transferred into a 500 mL flask equipped with a condenser and was refluxed with vigorous stirring at 90 °C for 9 h. After cooling to room temperature the mixture was subjected to vacuum filtration using a 0.2 μm millipore polycarbonate membrane filter that was then washed several times with distilled water until the pH of the filtrate was 7.0. The filtered solid was dried under vacuum for 24 h at 60 °C to give MWCNTs functionalized with carboxylic acid (MWCNTs-COOH).

2.3. Acylation of MWCNTs

MWCNTs-COOH (125 mg), synthesized as described above, was reacted with 100 mL of $SOCl_2$ at 70 °C for 24 h under reflux to convert the surface-bound carboxylic acid groups into acyl chloride groups. Any residual $SOCl_2$ was removed by rotary evaporation, and the solids that were subsequently obtained were filtered and washed with anhydrous THF. Lastly, the filtrate was dried under vacuum at room temperature for 4 h to give acyl chloride-functionalized MWCNTs (MWCNTs-COCl).

2.4. Synthesis of PANI functionalized MWCNTs composites (MWCNTs-*f*-PANI)

MWCNTs-COCl was reacted with DABSA under reflux in THF solvent at 60 °C for 48 h under a nitrogen atmosphere. The products were then separated by centrifugation, washed well with methanol, and dried under vacuum at room temperature. The resultant product was designated MWCNTs-DABSA.

The synthesis procedure of MWCNTs-*f*-PANI was as follows: MWCNTs-DABSA was dispersed in 20 mL of a 0.5 M HCl containing 2.7 mmol of aniline and stirred under ultrasonication conditions for 15 min. Next, 10 mL of APS solution (0.5 g) was added dropwise to the above mixture and the reaction was allowed to continue while

stirring at room temperature for 12 h. Unwanted byproducts in the precipitate were removed by washing with an excess of distilled water and methanol until the filtrate was colorless; the resulting filtrate was then dried under vacuum. The nanocomposite obtained was designated MWCNTs-*f*-PANI. For comparative purpose, pristine PANI was synthesized using the MWCNTs-*f*-PANI synthesis protocol but without using MWCNTs-DABSA.

2.5. Dispersion of Au or Ag nanoparticles into PANI functionalized carbon nanotubes (MWCNTs-*f*-PANI/Au or Ag-NC)

In a typical procedure, MWCNTs-*f*-PANI was dispersed in 40 mL of twice-distilled water containing 1 wt.% of $HAuCl_4{\cdot}H_2O$ and sonicated for 20 min. This mixture was then transferred to a round-bottom flask and heated to boiling while stirring, after which a 1 mL solution of sodium citrate was added, and ultrasonic stirring was continued for an additional 30 min. After the reaction was complete, the product, which was designated MWCNTs-*f*-PANI/Au-NC, was collected by centrifugation and dried overnight at 50 °C under vacuum. A similar procedure was followed for synthesis of MWCNTs-*f*-PANI/Ag-NC using $AgNO_3$ instead of $HAuCl_4{\cdot}H_2O$.

2.6. Characterization

Fine powdered samples were characterized using several techniques. High resolution transmission electron microscopy (HRTEM) studies were carried out with a Hitachi HF-2000 with an accelerating voltage of 200 kV. The sample was initially dispersed in ethanol by ultrasonication for 5 min. Afterwards, a drop of the suspension was transferred onto a carbon coated copper grid and mounted on the microscope, and the micrographs were recorded. Fourier transform infrared (FT-IR) spectra of the samples were obtained using a Bruker IFS 66v Fourier transform infrared spectrometer. UV–visible spectra were obtained using a Beckman UV–visible (DU 7500) spectrophotometer with a scanning speed of 200 nm/min and bandwidth of 0.1 nm. Wide-angle X-ray diffractograms (WAXD) were obtained on a Rigaku Geiger Flex D-Max III, using Ni-filtered Cu Kα radiation (40 kV, 15 mA) and a scanning rate of 0.05°/min.

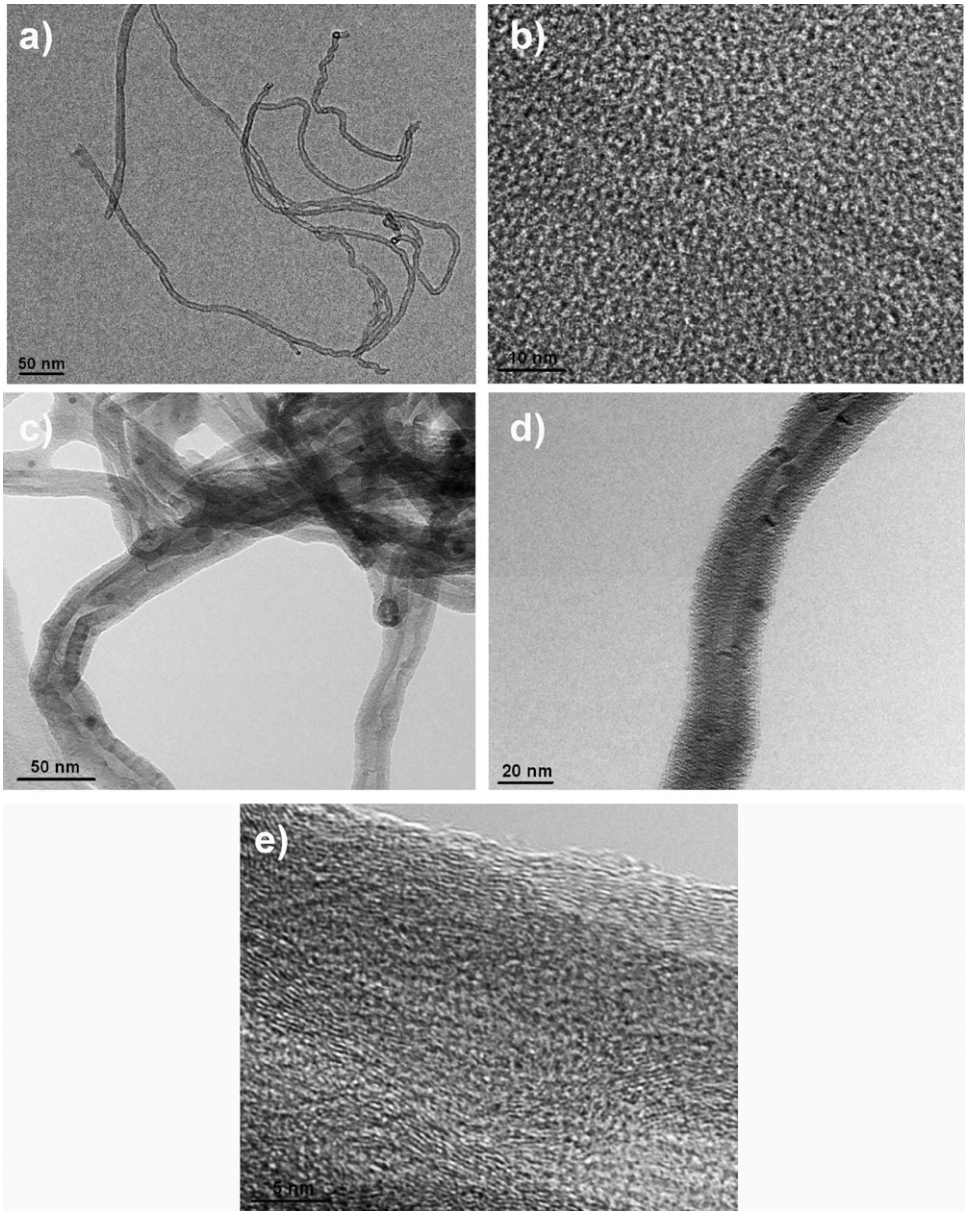

Fig. 1. Low and high magnification HRTEM images of the (a and b) oxidized MWCNTs; (c–e) MWCNTs-*f*-PANI.

The room temperature electrical conductivity of the polymers and composites were measured using a standard Van Der Pauw dc four-probe method [33].

3. Results and discussion

3.1. Morphology and formation of the MWCNTs-f-PANI/Au or Ag nanocomposites

The morphology and size of the as-oxidized MWCNTs, MWCNTs-*f*-PANI and MWCNTs-PANI/Au or Ag composites were investigated by HRTEM. Fig. 1a shows that after treatment of MWCNTs with mixtures of HNO_3 and H_2SO_4 under reflux, the nanotubes were opened, oxidized and shortened, and exhibited regular morphology. The nanotube dimensions were several hundred nanometers in length and 15–25 nm in diameter. As shown in Fig. 1c, MWCNTs were covered by PANI, indicating that the polymer was attached strongly to the CNTs. The difference between the high magnification HRTEM images of the purified CNTs (Fig. 1b) and MWCNTs-*f*-PANI (Fig. 1d and e) also clearly indicates that the carbon nanotubes were encapsulated by ordered PANI chains. In addition, it can be clearly seen from Figs. 2 and 3 that the 10–15 nm size of the metal (Au and Ag) nanoparticles were uniformly and individually distributed in the MWCNTs-*f*-PANI composite.

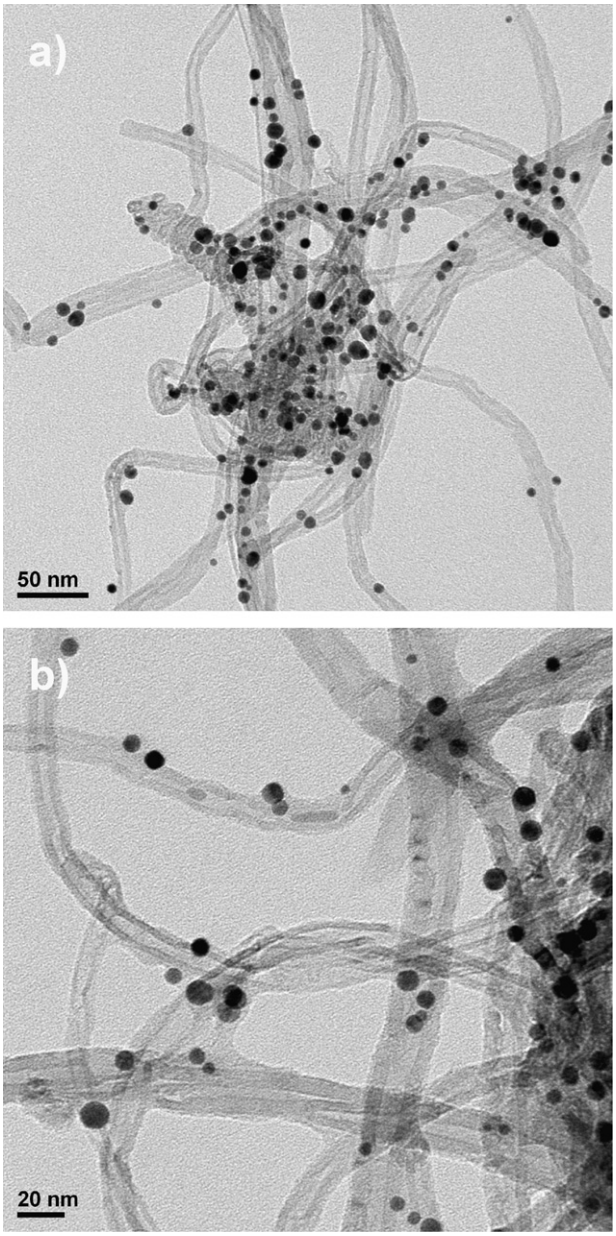

Fig. 2. (a and b) Low and high magnification HRTEM images of the MWCNTs-*f*-PANI/Au composites.

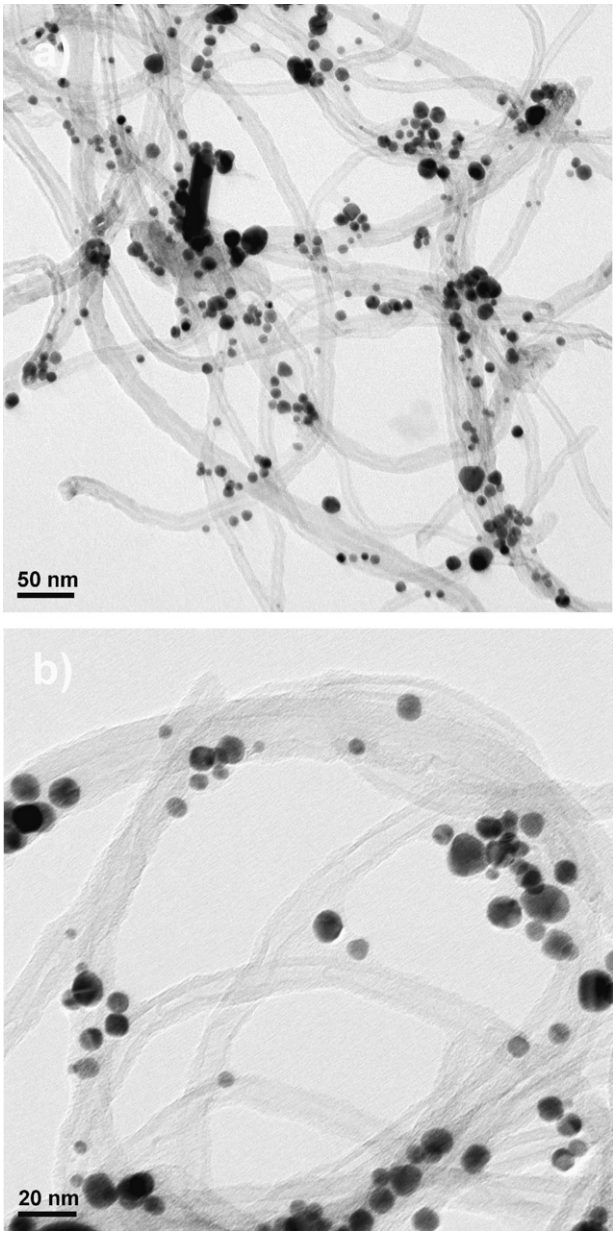

Fig. 3. (a and b) Low and high magnification HRTEM images of the MWCNTs-*f*-PANI/Ag composites.

The mechanism of MWCNTs-*f*-PANI/Au or Ag nanocomposite formation is shown in Scheme 1 and comprises the following steps: (i) purification and oxidation of pristine MWCNTs, (ii) conversion of MWCNTs to MWCNTs-COCl by reacting oxidized CNTs with acyl chloride, (iii) reaction of MWCNTs-COCl with DABSA via amide functionality, iv) reaction of active $-NH_2$ sites with an aniline monomer-oxidant solution to produce MWCNTs-*f*-PANI, and lastly, (v) dispersion of Au or Ag nanoparticles into MWCNTs-*f*-PANI.

It is well known that pure CNTs have both poor solubility and dispersibility, traits that result in their tendency to bundle up easily because of strong inter-tube van der Waals interactions. Like-

wise, hydrophobic interactions in aqueous solutions tend to retard alignment of CNTs. Such interactions of CNTs can be reduced by functionalization with DABSA to improve dispersibility. Indeed, we found that after functionalization of CNTs with DABSA, the nanotubes were well dispersed in the acidic solution containing aniline monomer. This increase in dispersibility may have also contributed to the improved electrical conductivity of the composite. Because DABSA functionalized MWCNTs possess a reactive $-NH_2$ group, they were simultaneously oxidized with aniline in APS solution to generate amine cation radicals for polymerization initiation, resulting in grafting of PANI chains onto the CNTs. Since Au and Ag are good electrical conductors, the electrical conductivity of the MWCNTs-*f*-PANI could be further improved by dispersion of the noble metal nanoparticles, thus providing a more effective electrical pathway. Upon addition of metal (Au or Ag) salt to a suspension of MWCNTs-*f*-PANI in aqueous solution, the metal ions were effectively absorbed under ultrasonication and were subsequently reduced to individual metal (Au or Ag) nanoparticles by the addition of sodium citrate, which acts as both a stabilizing and reducing agent. We employed ultrasonication to prevent the particles from aggregating with each other, resulting in the formation of high quality individual nanoparticles. Thus, most of the synthesized metal nanoparticles were well dispersed into MWCNTs-*f*-PANI, and no free metal nanoparticles were observed in the HRTEM images (Figs. 2 and 3). The formation of Au or Ag nanoparticles in the MWCNTs-*f*-PANI was attributed charge–charge electrostatic interactions between nitrogen sites present in MWCNT-*f*-PANI and negatively charged metal particles. We next characterized the structural, optical, and electrical properties of the composites.

3.2. X-ray diffraction analysis

X-ray diffraction patterns were analyzed to compare the crystallinity of the polymers and composites. Fig. 4 shows the X-ray diffraction patterns of (a) oxidized MWCNTs, (b) pristine PANI, (c) MWCNTs-*f*-PANI, (d) MWCNTs-*f*-PANI/Au, and (e) MWCNTs-*f*-PANI/Ag composites. Oxidized MWCNTs (Fig. 4a) exhibited a sharp, high intensity peak at $2\theta = 26^\circ$ and two lower intensity peaks at 43.4° and 54.1°, all of which were attributed to the diffraction signature of the distance between the walls of CNTs and the inter-wall spacing [34]. The pristine PANI (Fig. 4b) exhibited peaks at $2\theta = 14.8^\circ$, 20.95°, and 25.92°, which were ascribed to the periodicity parallel and perpendicular to the polymer chains, respectively [35]. For MWCNTs-*f*-PANI (Fig. 4c) the X-ray pattern showed both the characteristic peaks of PANI and the peaks of CNTs. In addition, the intensity of the diffraction peak of PANI in MWCNTs-*f*-PANI at 26° was significantly increased due to structural ordering of PANI on the surface of the CNTs; this observation confirmed that the synthesis of MWCNTs-*f*-PANI was successful.

The diffraction pattern of the MWCNTs-*f*-PANI/Au or Ag composites were different from that of the oxidized MWCNTs, pristine PANI, and MWCNTs-*f*-PANI. A few additional diffraction peaks at approximately 39°, 44°, 64° and 77° were observed for the nanocomposites, representing Bragg's reflections from (1 1 1), (2 0 0), (2 2 0) and (3 1 1) planes of Au or Ag nanoparticles, respectively. These peaks were matched with JCPDS data of crystalline Au or Ag [36–38]. The XRD results suggest that MWCNTs-*f*-PANI/Au or Ag-NCs were more crystalline than pristine PANI and MWCNTs-*f*-PANI due to the presence of crystalline Au or Ag nanoparticles. The average size of the Au or Ag nanoparticles was estimated using Scherrer's equation [39]:

$$L = \frac{0.9\lambda}{\beta_{(2_\theta)}} \cos\theta_{\max}$$

where L is the mean size of the metal nanoparticles, λ is the wavelength of the X-ray source ($\lambda_{(Cu,\,K\alpha)} = 1.5418$ Å), $\theta_{\max}$ is the angle at peak maximum (in radians) of a chosen XRD peak, and $\beta_{(2\theta)}$ is the full-width at half-maximum of the chosen XRD peak. The reflecting peak at (1 1 1) was used to estimate the average size (~15 nm) of the Au or Ag nanoparticles, and was consistent with HRTEM results. The content of the CNT, Au and Ag nanoparticles in the composites were 20.74, 4.38 and 4.51 wt.%, respectively, as measured using thermogravimetric analysis (data not shown).

3.3. Structural characterization

FT-IR spectra were used to characterize the functional groups of polymers and CNTs after modification. Fig. 5 shows the FTIR spectra of (a) oxidized MWCNTs, and (b) pristine PANI, (c) MWCNTs-*f*-PANI, (d) MWCNTs-*f*-PANI/Au, and (e) MWCNTs-*f*-PANI/Ag composites. Oxidized MWCNTs (Fig. 5a) generated a weak peak at 1725 cm^{-1}, which was due to the carbonyl stretch of the carboxylic acid group. Pristine PANI (Fig. 5b) showed absorption bands at 1573 cm^{-1} (C=C stretching deformation of quinoid), 1482 cm^{-1} (benzenoid ring), 1297 cm^{-1} (C–N stretching vibration), 1131 cm^{-1} (N=Q=N, Q is quinoid), and 809 cm^{-1} (C–H out of plane bending vibration) [40], where N=Q=N was used as a measure of electrons delocalization. The spectrum of MWCNTs-*f*-PANI (Fig. 5c) was quite different. For MWCNTs modified with PANI, a new band appeared at 1660 cm^{-1},

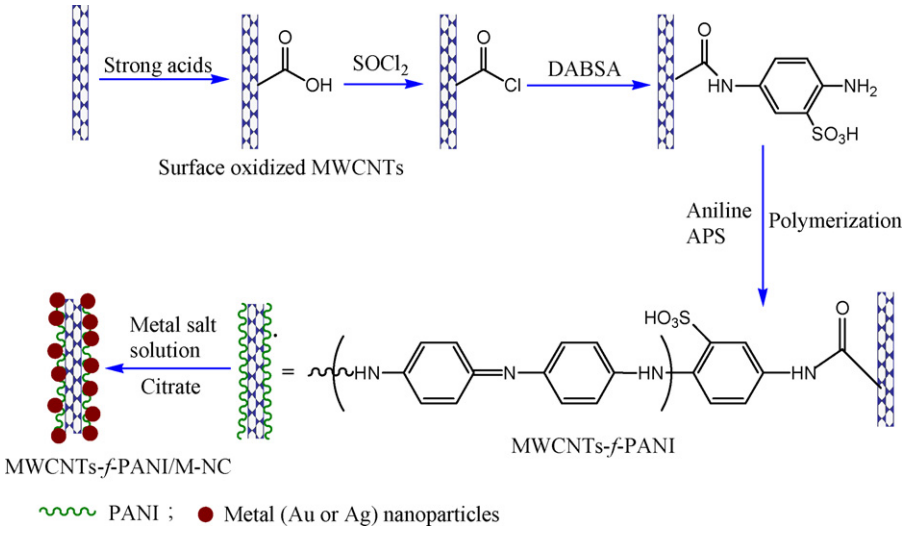

Scheme 1. Schematic illustration of the synthesis of MWCNTs-*f*-PANI/M (M = Au or Ag) nanocomposites.

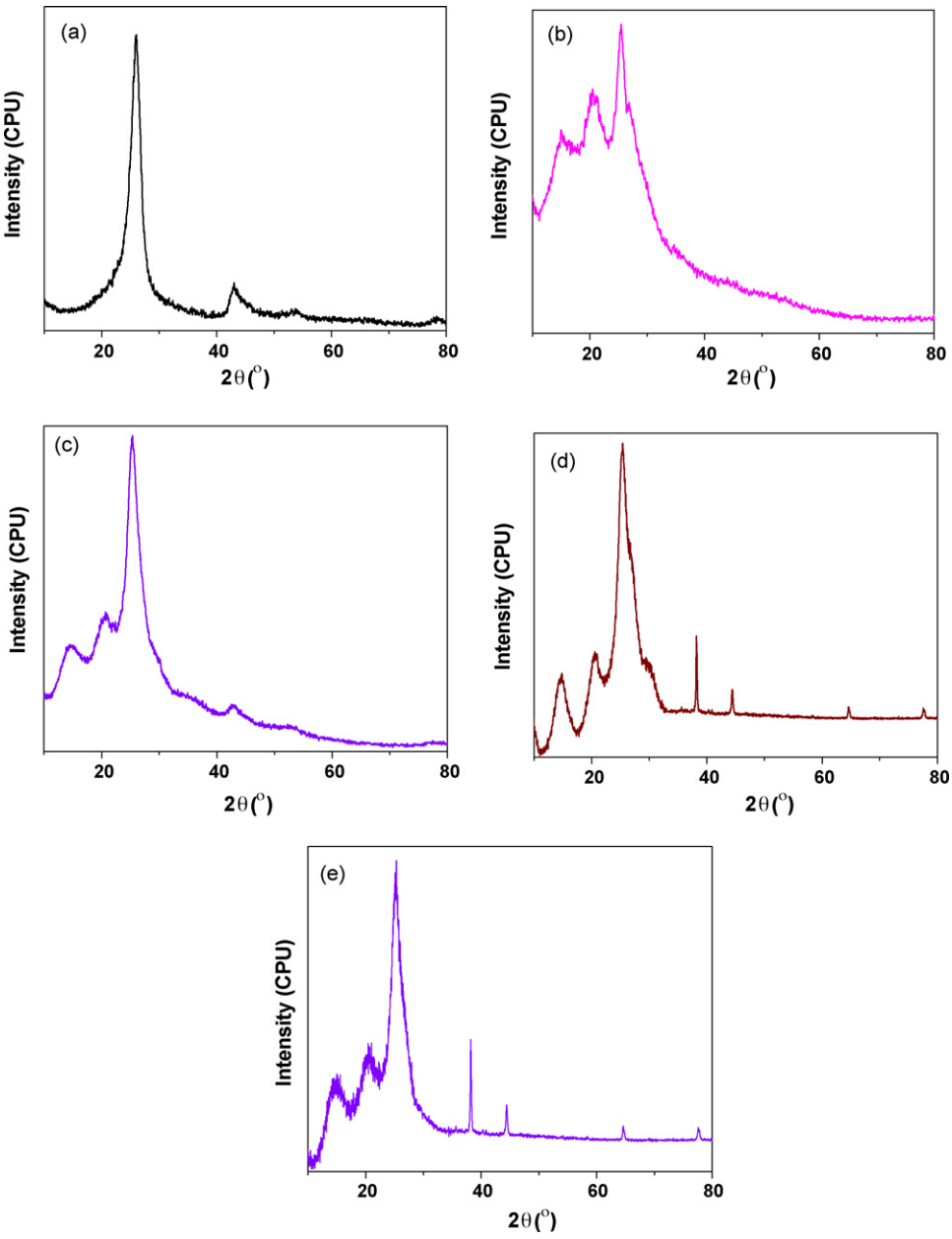

Fig. 4. XRD patterns of the (a) oxidized MWCNTs, (b) pristine PANI, (c) MWCNTs-*f*-PANI, (d) MWCNTs-*f*-PANI/Au, and (e) MWCNTs-*f*-PANI/Ag composites.

which was attributed to the carbonyl stretch of the amide. In addition, the absorbance at 1725 cm^{-1} typically seen with CNTs was absent (Fig. 5c), indicating that the reaction with –COOH and formation of amides was complete. In addition, new strong peak that appeared around 1040 cm^{-1} was ascribed to the $-SO_3H$ group, which arose from the incorporation of DABSA. Together, these results supported our hypothesis that PANI would become covalently functionalized to the MWCNTs via the formation of an amide bond. Similarly, these bands were present in the spectra of the MWCNTs-*f*-PANI/Au or Ag NCs (Fig. 5d and e). Also, the absorption peak of C=C of the quinoid ring at 1130 cm^{-1} was red shifted by ~15 cm^{-1} for the composites because of strong electrostatic interaction between metal particles and PANI functionalized MWCNTs, indicating that there was an effective increase in the degree of electron delocalization that in turn enhanced the conductivity of the polymer chains. According to elemental analysis results, nanocomposites have S/N values around 0.2 indicates that presence of $-SO_3H$ group in the composites.

3.4. UV–visible spectra analysis

A UV–visible spectrum was used to investigate the electronic properties of MWCNTs, polymer and composites. As shown in Fig. 6a, no absorption peaks were observed for oxidized MWCNTs in the range of 300–800 nm while pristine PANI (Fig. 6b) exhibited two bands, with one peak at 320 nm attributed to π–π^* transitions in the bezenoid units of the polymer chain and the second peak at 610 nm attributed to exciton-like transitions in quinoid units [41]. In addition, the MWCNTs-*f*-PANI (Fig. 6c) peaks were similar to the peaks of PANI, albeit with some minor shifting of each characteristic peak, indicating that the resultant polymer was stable. The presence of noble metal particles in the MWCNTs-*f*-PANI was also confirmed using UV–visible spectroscopy. Specifically, when the nanocomposites (Fig. 6d and e) were formed, additional absorption peaks appeared at around 530 and 420 nm, which corresponds to the surface plasmon resonance of Au and Ag nanoparticles [37,42]. Fig. 6d shows that the intensity of Au absorption was higher than

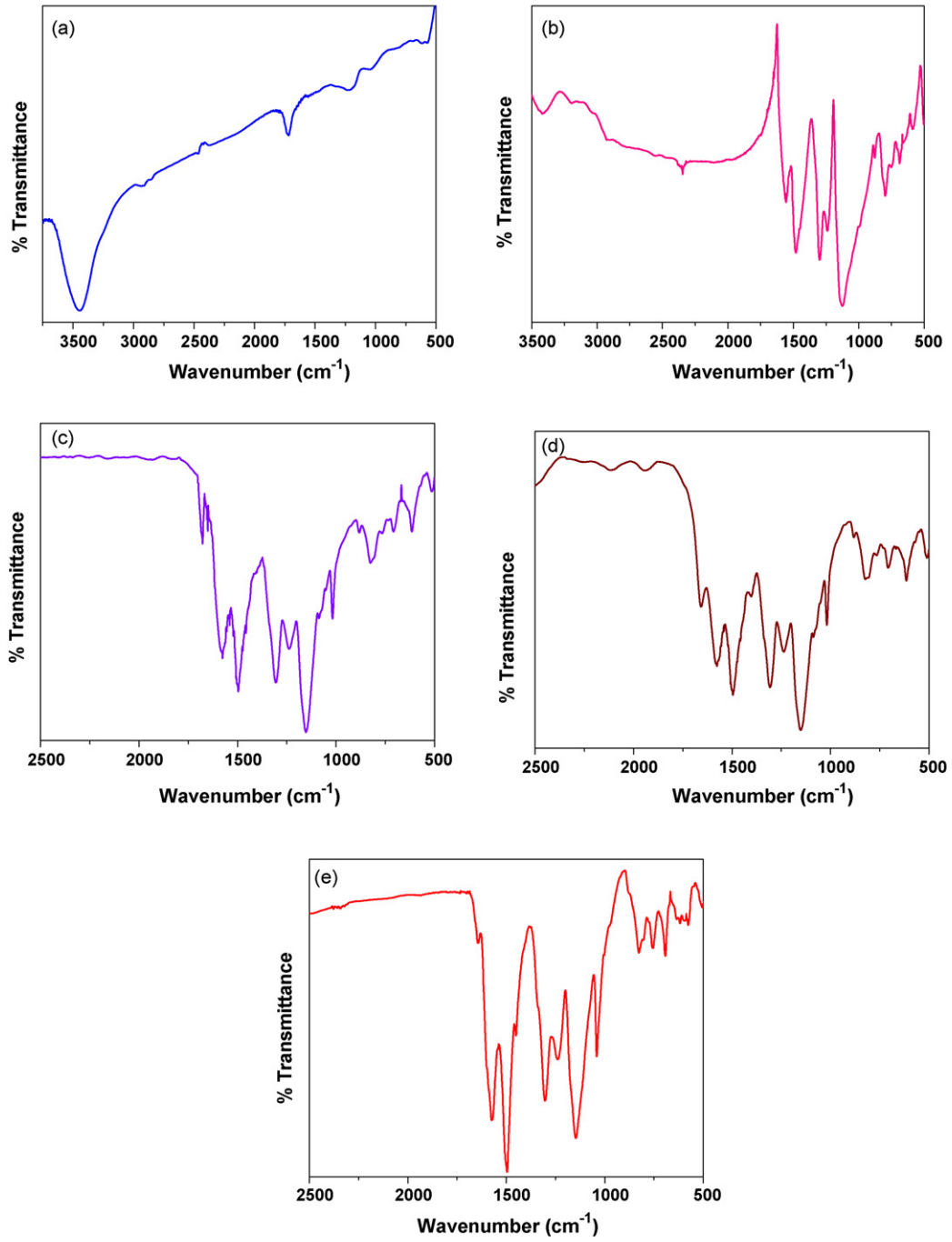

Fig. 5. FT-IR spectra of the (a) oxidized MWCNTs, (b) pristine PANI, (c) MWCNTs-*f*-PANI, (d) MWCNTs-*f*-PANI/Au, and (e) MWCNTs-*f*-PANI/Ag composites.

that of Ag in the composites. The intensity of the metal absorption bands changed due to their surface plasmon resonance, as these bands are sensitive to various parameters such as size and shape, dielectric constant of the medium and interparticle interactions [43]. In addition, the benzenoid and quinoid absorption bands observed for MWCNTs-*f*-PANI were slightly shifted to a smaller wavelength in the nanocomposites, indicating an interaction between the metal nanoparticles and nitrogen sites in PANI functionalized CNTs. This result was also supported by data from the FT-IR and XRD. Lastly, we examined the dispersibility of the composites in different solvents. The composites were well dispersed in several organic solvents, including DMF, THF and $CHCl_3$.

3.5. Electrical conductivity

The room temperature electrical conductivities of pristine PANI, MWCNTs-*f*-PANI, MWCNTs-*f*-PANI/Au-NC, and MWCNTs-*f*-PANI/Ag-NC were 2.5×10^{-3}, 0.18, 4.79 and 5.04 S/cm, respectively. MWCNTs-*f*-PANI had a higher conductivity than pristine PANI due to the large aspect ratio and surface area of CNTs, which likely facilitated an efficient charge transport between the PANI and CNTs. The conductivity of the simple, non-functionalized MWCNTs-PANI composite was 9.3×10^{-3} S/cm. Surprisingly, the conductivity of the MWCNTs-*f*-PANI was higher than that of the MWCNTs-PANI composite prepared without functionalization. It is clear that the significant improvement was ascribed to functionalization of

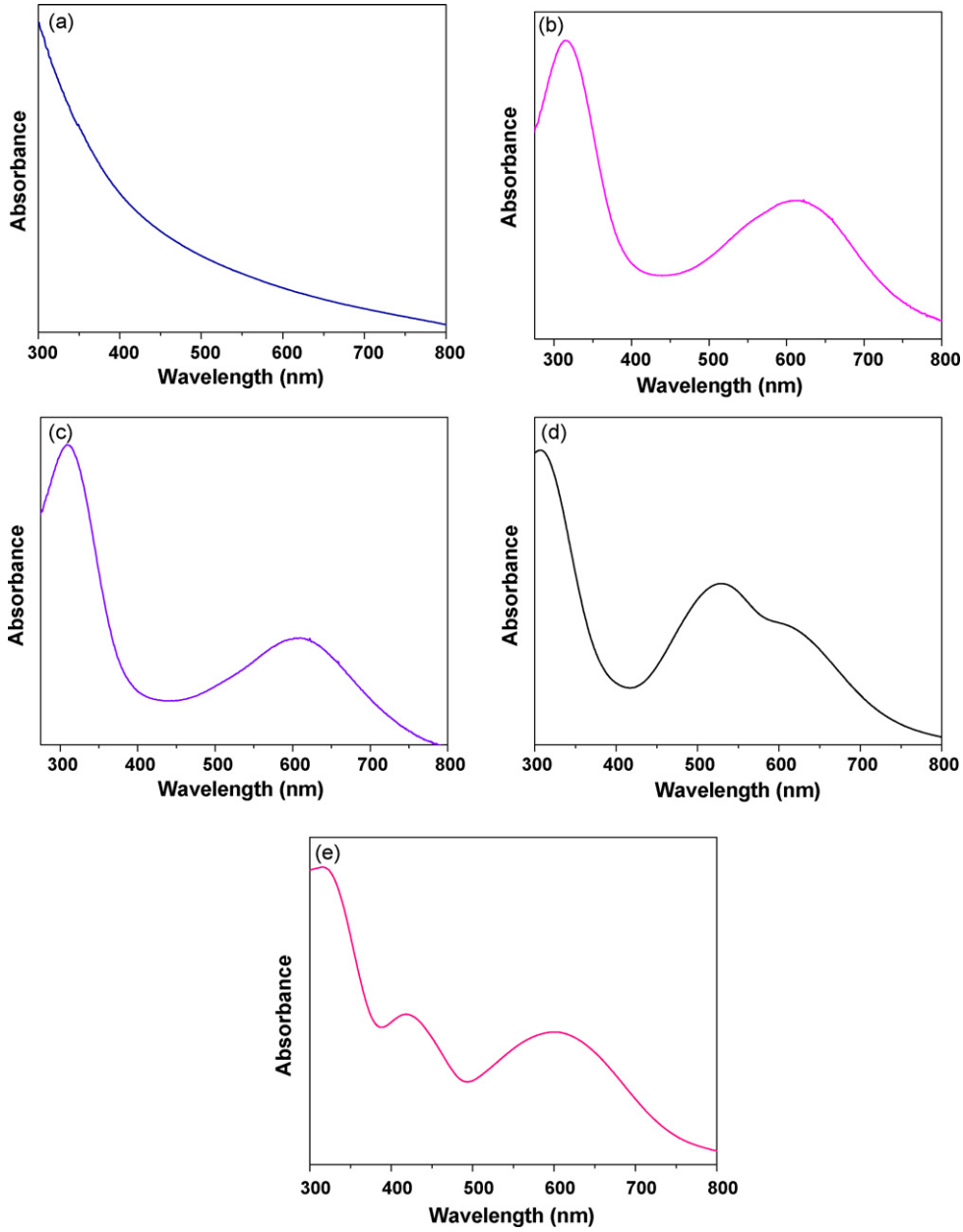

Fig. 6. UV–vis spectra of the (a) oxidized MWCNTs, (b) pristine PANI, (c) MWCNTs-*f*-PANI, (d) MWCNTs-*f*-PANI/Au, and (e) MWCNTs-*f*-PANI/Ag composites.

MWCNTs, as the strong chemical bonding between PANI and MWCNTs enhanced delocalization of charges and charge carrier mobility. The above results clearly demonstrate that functionalization is an effective method to enhance interfacial adhesion and achieve sufficient charge transfer from CNTs to a polymer. Upon dispersion into metal (Au or Ag) nanoparticles, the conductivity of the MWCNTs-*f*-PANI was greatly enhanced because: (i) effective dispersion of Au or Ag nanoparticles favors electronic transport and (ii) there was an enhancement of crystallinity in the composites as observed from XRD results.

4. Conclusions

We have demonstrated a facile approach to the synthesis of PANI functionalized MWCNTs containing noble metal (gold and silver) nanoparticles. At first, *in situ* chemical oxidative graft polymerization was employed to functionalize MWCNTs with PANI. Next, Au and Ag nanoparticles were dispersed into the MWCNTs-PANI by reducing the respective metal ions with citrate. The structures of the resulting nanocomposites were characterized by HRTEM, FT-IR, UV–vis and XRD. HRTEM results revealed that Au or Ag nanoparticles of approximately 15 nm in size were well distributed in the composites. FT-IR spectra showed that PANI had been covalently bonded to the MWCNTs via amide functionality. UV–vis absorption spectra showed surface plasmon resonance absorption bands at 530 and 410 nm, indicating that Au and Ag nanoparticles were indeed present in the composites. Covalently functionalized MWCNTs-*f*-PANI exhibited higher conductivity than that of pristine PANI and 'non-covalent' simple MWCNTs-PANI composites due to strong interactions between functional CNTs and PANI. Further, the conductivity of the CNTs-*f*-PANI was significantly enhanced following loading of the metal nanoparticles. This versatile method could be extended to synthesis of other polymer-functionalized CNTs with various metal nanoparticles. Such novel hybrid nanocomposites may find potential applications in various fields, such as nanoelectronics, catalysis, fuel cells, sensors, and photovoltaic devices.

Acknowledgement

This work was supported by the Research Fund of the University of Ulsan.

References

[1] S. Iijima, T. Ichihashi, Nature 363 (1993) 603.
[2] R.H. Baughman, A.A. Zakhidov, W.A. de Heer, Science 297 (2007) 787.
[3] H.J. Choi, K. Zhang, J.Y. Lim, J. Nanosci. Nanotechnol. 7 (2007) 3400.
[4] K.R. Reddy, B.C. Sin, C.H. Yoo, W. Park, K.S. Ryu, J.S. Lee, D. Sohn, Y. Lee, Scr. Mater. 58 (2008) 1010.
[5] M.S. Dresselhaus, G. Dresselhaus, P.C. Eklund, Science of Fullerenes and Carbon Nanotubes, Academic Press, San Diego, 1996.
[6] C.N.R. Rao, B.C. Satishkumar, A. Govindaraj, M. Nath, Chem. Phys. Chem. 2 (2001) 78.
[7] J. Liu, A.G. Rinzler, H. Dai, J.H. Hafner, R.K. Bradley, P.J. Boul, A. Lu, T. Iverson, K. Shelomov, C.B. Huffman, F. Rodriguez-Macias, Y.S. Shon, T.R. Lee, D.T. Colbert, R.E. Smalley, Science 280 (1998) 1253.
[8] J. Chen, M.A. Hammon, H. Hu, Y.S. Chen, A.M. Rao, P.C. Eklund, R.C. Haddon, Science 282 (1998) 95.
[9] C.Y. Hong, Y.Z. You, C.Y. Pan, J. Polym. Sci. Part A: Polym. Chem. 44 (2006) 1941.
[10] S.H. Jin, D.S. Lee, J. Nanosci. Nanotechnol. 7 (2007) 3847.
[11] M. Kim, C.K. Hong, S. Choe, S.E. Shim, J. Polym. Sci. Part A: Polym. Chem. 45 (2007) 4413.
[12] J.Y. Jeong, H.J. Lee, S.W. Kang, L.S. Tan, J.B. Baek, J. Polym. Sci. Part A: Polym. Chem. 46 (2008) 6041.
[13] K.R. Reddy, K.P. Lee, A.I. Gopalan, H.D. Kang, React. Funct. Polym. 67 (2007) 943.
[14] R. Aitout, A. Belgaid, L. Maksloufi, B. Saidani, React. Funct. Polym. 66 (2006) 373.
[15] R.K. Mohammad, T.L. Kwan, C.J. Lee, T.I. Bhuiyan, H.J. Kim, L.S. Park, M.S. Lee, J. Polym. Sci. Part A: Polym. Chem. 45 (2007) 5741.
[16] K.R. Reddy, K.P. Lee, A.I. Gopalan, A.M. Showkat, Polym. Adv. Technol. 18 (2007) 38.
[17] M.R. Karim, C.J. Lee, Y.T. Park, M.S. Lee, Synth. Met. 151 (2005) 131.
[18] J. Oh, M.E. Kozlov, B.G. Kim, H.K. Kim, R.H. Baughman, Y.H. Hwang, Synth. Met. 15 (2008) 638.
[19] M.R. Karim, C.J. Lee, M.S. Lee, J. Polym. Sci. Part A: Polym. Chem. 44 (2006) 5283.
[20] F. Qu, M. Yang, J. Jiang, G. Shen, R. Yu, Anal. Biochem. 344 (2005) 108.
[21] A.A. Anjali, S.V. Bhagwat, P.P. Katre, Sens. Actuators B: Chem. 114 (2006) 263.
[22] S. Satyanarayanan, S.S. Azim, G. Venkatachari, Synth. Met. 157 (2007) 205.
[23] K.R. Reddy, K.P. Lee, A.I. Gopalan, J. Nanosci. Nanotechnol. 7 (2007) 3117.
[24] R. Bissessur, K.Y. Liu, W. White, S. Scully, Langmuir 22 (2006) 1729.
[25] Y.P. Zhang, S.H. Lee, K.R. Reddy, A.I. Gopalan, K.P. Lee, J. Appl. Polym. Sci. 104 (2007) 2743.
[26] Z. Liu, J. Zhou, H. Xue, L. Shen, H. Zang, W. Chen, Synth. Met. 156 (2006) 721.
[27] J.R. Skotheim, R.L. Elsenbaumer, J.R. Reynolds, Handbook of Conducting Polymers, 2nd edn., Marcel Dekker, NY, 1998.
[28] A.G. MacDiarmid, Angew. Chem. Int. Ed. 40 (2001) 2581.
[29] W.L. Barnes, A. Dereux, T.W. Ebbesen, Nature 424 (2003) 824.
[30] T. Shimada, K. Ookubo, N. Komuro, T. Shimizu, N. Uehara, Langmuir 23 (2007) 11225.
[31] S.K. Pillalamarri, F.D. Blum, A.T. Tokuhiro, M.F. Bertino, Chem. Mater. 17 (2005) 5941.
[32] K. Mallick, M.J. Witcomb, A. Dinsmore, M.S. Scurrell, Macromol. Rapid Commun. 26 (2005) 232.
[33] L.J. Van Der Pauw, Philips Res. Rep. 13 (1958) 1.
[34] Y. Saito, T. Yoshikawa, S. Bandow, M. Tomita, T. Hayashi, Phys. Rev. B 48 (1993) 1907.
[35] J.P. Pouget, Jozefowicz, A.J. Epstein, X. Tang, A.G. MacDiarmid, Macromolecules 24 (1991) 779.
[36] B.D. Cullity, Elements of X-ray Diffraction, Addison-Wesley, Reading, MA, 1978.
[37] P. Dallas, D. Niarchoas, D. Vrbanic, N. Boukos, S. Pejovnik, C. Trapalis, D. Petridis, Polymer 48 (2007) 2007.
[38] S.W. Kim, J. Park, Y. Jang, Y. Chung, S. Hwang, T. Hyeon, Y.W. Kim, Nanoletters 3 (2003) 1289.
[39] H.P. Klug, L.E. Alexander, X-ray Diffraction Procedures for Polycrystalline and Amorphous Materials, Wiley, New York, 1954.
[40] K.G. Neoh, E. Tang, K.L. Tan, Synth. Met. 60 (1993) 13.
[41] Y.H. Kim, C. Foster, J. Chiang, A.J. Heeger, Synth. Met. 29 (1989) 285.
[42] B. Li, C.Y. Li, J. Am. Chem. Soc. 129 (2007) 12.
[43] C.A. Mirkin, Inorg. Chem. 39 (2000) 2258.